

Screening and Identification of Salicin Compound from *Desmodium gangeticum* and its *In vivo* Anticancer Activity and Docking Studies with Cyclooxygenase (COX) Proteins from *Mus musculus*

Preeti Srivastava^{1*}, Vinay K Singh¹, Brahma Deo Singh¹, Gaurava Srivastava², Bhuwan B Misra³ and Vyasji Tripathi³

¹School of Biotechnology, Faculty of Science, Banaras Hindu University, Varanasi-221005, Uttar Pradesh, India

²School of Biochemical Engineering, Indian Institute of Technology, Banaras Hindu University, Varanasi-221005, Uttar Pradesh, India

³Department of Chemistry, Faculty of Science, Banaras Hindu University, Varanasi-221005, Uttar Pradesh, India

Abstract

Cancer continues to be a worldwide killer, despite the enormous amount of research and rapid developments seen during the past decade. It has been suggested that by 2020 more than 15 million new cases of cancer will be diagnosed. Since it is commonly believed that many are preventable, there is urgent need to identify/develop natural medicines as effective chemopreventive agents. The purpose of this current study was to assess the effect of isolated and characterized salicin on cyclooxygenase (COX) proteins by molecular docking studies and by assessments of the effects of drug-ligand interaction. Salicin isolated from *Desmodium gangeticum*, a medicinal legume, is a COX inhibitor. The present study reports the extraction, isolation and identification of salicin and its interaction with COX-1 and COX-2 derivatives, which may be useful for drug-designing for anti-cancer activities. Molecular modeling and docking studies revealed the binding orientations of salicin into the active sites of COX-1 and COX-2 enzymes. Extraction, isolation and characterization of the compound 2-(hydroxymethyl) phenyl hexopyranoside, also known as 'salicin', from the leaves of *D. gangeticum* first time. Anticancer evaluation of salicin in *in vivo* mice model.

Keywords: Cyclooxygenase; Salicin; Docking; Molecular modeling; Functional motif; Anti-cancer; *Desmodium gangeticum*

Abbreviations: COX: Cyclooxygenase; nM: Nanomolar; NSAID: Nonsteroidal Anti-Inflammatory Drug; DG: *Desmodium Gangeticum*

Introduction

Plants have been utilized as medicines for thousands of years [1], initially as crude drugs like tinctures, teas, poultices, powders and other herbal formulations [1,2]. The identity medicinal plants and the methods of their use were passed down through oral history, but eventually this information was recorded in herbals, and subsequently active compounds were isolated beginning with morphine from opium in the early 19th century [1,3], followed by cocaine, codeine, digitoxin and quinine [1,4,5]. Isolation and characterization of pharmacologically active compounds from medicinal plants continue today, and drug discovery techniques are now being used to standardize herbal medicines and to elucidate analytical marker compounds. Methods used to acquire compounds for drug discovery include isolation from plants and other natural sources, chemical synthesis, combinatorial chemistry and molecular modeling [6-8]. Drug discovery from medicinal plants has contributed to cancer treatment, and most new clinical applications during the last half century relate to cancer [4,5,9]. By 2020, approximately 15 million new cancer cases will be diagnosed, and 12 million these patients will die [10]. Cancer is caused by both internal factors such as inherited mutations, hormones, and immune conditions, and environmental/acquired factors like tobacco, diet, radiation, and infectious organisms [11]. The attractiveness of natural compounds as drugs partly stems from their potential ability to influence multiple components of the carcinogenesis pathway.

Natural products are typically isolated in quantities insufficient for lead optimization, lead development, and clinical trials. Therefore, possibilities of their synthesis or semi-synthesis need to be explored [8,12]. In addition, libraries of natural products and natural-product-like compounds including their features important for combinatorial chemistry may be created [13-15].

There are two well established isoforms of the cyclooxygenase (COX) enzyme that differ in their distribution in the body and in physiological function. COX-1 is constitutively expressed in normal tissues and it is involved in maintaining mucosal integrity, platelet aggregation and gastric cytoprotection [16]. In contrast, COX-2 is not expressed in normal mucosa, but is expressed very early in response to neoplastic and inflammatory stimuli, and is extensively overexpressed in different neoplasms, making it an attractive therapeutic target. Besides the role of COX-2 in the production of inflammatory prostaglandins, its momentous participation in the initiation/propagation of cancer [17-21] and in the development of multidrug resistance is well explored [22,23]. Over-expression of COX-2 probably occurs from the first genetically altered cell, through hyperplasia, dysplasia, carcinoma, and even metastasis of colorectal cancer [24-26]. Number of nonsteroidal anti-inflammatory drugs (NSAIDs) and selective COX-2 inhibitors have been investigated for anticancer activities [27-31].

Pharmacological inhibition of COX can provide relief from inflammation and, as a result, from pain. Non-steroidal anti-inflammatory drugs, such as aspirin and ibuprofen, exert their effects through inhibition of COX. Turmeric, ginger, boswellia, hops and some

***Corresponding author:** Preeti Srivastava, School of Biotechnology, Faculty of Science, Banaras Hindu University, Varanasi-221005, Uttar Pradesh, India, Tel: +91-9236060830; Fax: +91- 542-2368693; E-mail: preetibbhu@gmail.com

Received March 18, 2013; **Accepted** May 27, 2013; **Published** May 30, 2013

Citation: Srivastava P, Singh VK, Singh BD, Srivastava G, Misra BB, et al. (2013) Screening and Identification of Salicin Compound from *Desmodium gangeticum* and its *In vivo* Anticancer Activity and Docking Studies with Cyclooxygenase (COX) Proteins from *Mus musculus*. J Proteomics Bioinform 6: 109-124. doi:10.4172/jpb.1000269

Copyright: © 2013 Srivastava P, et al. This is an open-access article distributed under the terms of the Creative Commons Attribution License, which permits unrestricted use, distribution, and reproduction in any medium, provided the original author and source are credited.

plants exert their anti-inflammatory influences through inhibition of COX-2.

Desmodium gangeticum (L.) DC commonly known as shalparni or Ticktree is a member of Fabaceae, and is used in 'Ayurvedic' preparations like 'Dashmoolarishta' and 'Dashmoola kwaath' for the post-natal care to avoid secondary complications. In Indian system of medicine it is used as a bitter tonic, febrifuge, digestive, anticatarrhal, antiemetic, in inflammatory conditions of chest and various other inflammatory conditions due to vata disorder [32,33] and in treatment of abscess, acne, cataract, dysentery, eye diseases, infections and liver diseases [34]. Aqueous extract of this plant exhibits anti-inflammatory, severe antiwrithing activity, moderate central nervous system (CNS) depressant activity as well as antileishmanial, antibacterial and antifungal activities [34-38]. The ethanolic extract acts as a potent antiulcer agent in all models, mainly more due to its cryoprotective effect than anti-secretory effects [39]. The extracts show wound healing potential and antidiabetic activity [40,41]. *D. gangeticum* is reported to contain alkaloids, pterocarpenoids, flavones and isoflavanoid glycosides [42], and is supposed have anti-oxidant activities in its aerial parts [43]. The sterols *N, N*-dimethyltryptamine, 5-methoxy-*N, N* dimethyltryptamine, their oxides and other derivatives have been isolated from aerial parts [44]. Gangetin, a pterocarponoid from *D. gangeticum* has been shown to possess anti-inflammatory and analgesic activities [45].

White Willow Bark and Meadowsweet are sources of salicin, which has analgesic as well as anti-inflammatory properties. Salicylic acid, released from Salicin in the body, provides anti-inflammatory and pain-relieving actions [46], and the same COX-2 inhibition properties as aspirin, but unlike aspirin it does not function as an anticoagulant [47]. Salicin from white willow bark extract showed modest effectiveness in treating pain associated with knee and/or hip osteoarthritis [48] and back pain [49], when administered over a period of weeks in dose of up to 240 mg/day.

Our main objective is to optimize Salicin as a specific inhibitor of COX-1 and COX-2 enzymes in the hope that this molecule may be further explored as novel anticancer, especially anti-colorectal cancer, lead-candidates. As in our other report under *in vivo* condition salicin is proved a potent anticancer drug. Our strategy is intended to obtain selective inhibition of COX-2 using traditional medicinal chemistry techniques motivated by the comparative modeling of a COX-1 and COX-2 complexed with Salicin together with the available pharmacophore. The modern modeling and docking programs/software packages e.g. Discovery Studio module DS Modeler, Docking Server and Q-site Finder have been used to determine the active sites of COX-1 and COX-2 proteins. The structure of ligand against this active binding site can be found by Q-site Finder. The exact conformation and configuration of the ligand can be calculated to find the best molecule with minimum binding energy and it can be used to develop potential drug molecules against the disease. This knowledge may be important for the development of novel therapies for the treatment of infectious and other viral diseases in the future.

Material and Methods

Plant material

The plant *D. gangeticum* was collected in the month of Nov 2008 from Ayurvedic Garden, Institute of Medical Sciences, B.H.U, Varanasi. This plant occurs naturally on the lower hills and in the plains throughout India. The plants were taxonomically authenticated

at the site and collected locally and from surrounding areas as well as from the ayurvedic garden of Banaras Hindu University, Varanasi.

Isolation of Salicin

Dry and finely powdered leaves (5 kg) of *D. gangeticum* were extracted with methanol (6×5 L) for 36 h using a Soxhlet apparatus at 60-70°C. The residue (536 g) obtained after *in vacuo* concentration was further fractionated in n-hexane (2 L×2), chloroform (1 L×1), and ethyl acetate (1 L×3) using a mechanical stirrer followed by concentration under reduced pressure to afford crude residue of 152 g, 34 g and 92 g, respectively (Figure 1). Systematic chemical investigation of the methanolic leaf extract enabled isolation of known glycoside, 2-(hydroxymethyl)phenyl hexopyranoside (DG-1), also known as 'salicin' which is conventionally isolated from the willow bark [50]; this is the first report of isolation of salicin from leaves of *D. gangeticum*.

Ligand optimization

Salicin is a glycoside, which acts as a precursor for the synthesis of acetyl salicylic acid. For ligand molecule, the structure of salicin, SDF file was retrieved from PubChem site (<http://www.ncbi.nlm.nih.gov/pccompound>). Salicin.sdf file was converted into PDB file using Discovery Studio visualize and geometry was cleaned by 'clean geometry' menu of Discovery Studio 3.0 and saved for further computational analysis. This retrieved ligand file was imported to the Docking Server program for docking with COX-1 and COX-2 proteins of *Mus musculus* obtained from NCBI database sequence (<http://www.ncbi.nlm.nih.gov/>) for homology modeling using Discovery Studio 3.1 DS Modeler.

3D Preparation of receptor molecule

The amino acid sequence of COX-1 and COX-2 was used to search template structure using PDB Database (<http://www.pdb.org/pdb/home/home.do>). After getting the templates 1CQE with 85% similarity for COX-1 and 1CVU with 97% similarity for COX-2 (Figure 2), they were taken for homology modeling using Discovery Studio 3.1 module DS MODELER [51].

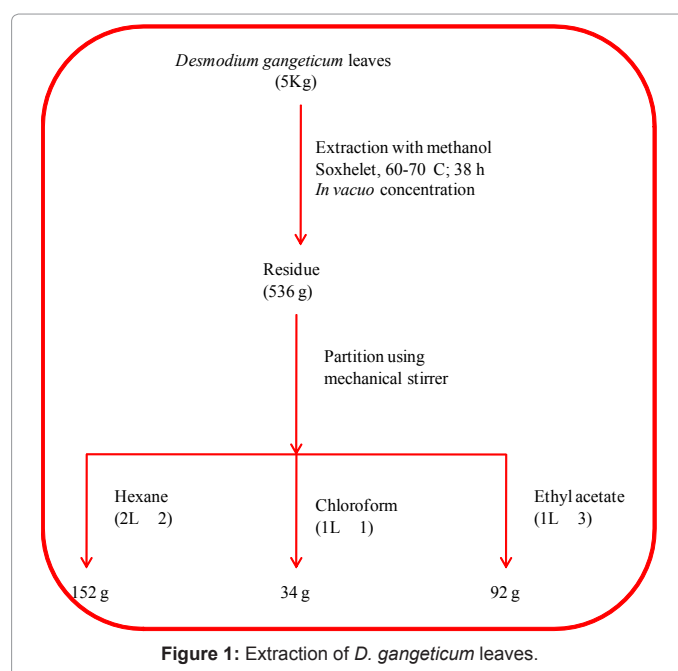


Figure 1: Extraction of *D. gangeticum* leaves.

Energy minimization

The 3D modeled structures of COX-1 and COX-2 were used for energy minimization using CHARMM force field based on Conjugate Gradient (CONJ) method that exhibits better convergence than the steepest descent method.

Validation of the modeled protein structures

The validity of protein models was tested using DS Protein Health tool, which verifies a protein structure derived from modeling studies or experimental methods. Profiles-3D Verify program based on Kabsch-Sander method was used to evaluate the likelihood that an amino acid should be present within its current environment. It allows us to browse and correct a suggested list of structural violations, which are mapped and colored to the 3D structure. Then CHARMM-based structural refinement of loops and side chains was performed using DS Protein Refine tool. LOOPER algorithm was used for loop refinement that quickly generated energy optimized variants of the structure and provided a list of proposed loop conformations that have been scored using the CHARMM Energy function. The stereochemical quality of modeled protein was checked by Ramchandaran plot provided by online PDBsum analysis. Model quality assessment was done using RAMPAGE (<http://mordred.bioc.cam.ac.uk/>). Qmean server (<http://swissmodel.expasy.org/qmean/cgi/index.cgi>) and quantitative evaluation of protein structure quality were done with VADAR (Volume, Area, Dihedral Angle Reporter) server (<http://vadar.wishartlab.com/>).

Calculating the active site sequence

Active site analysis was done using 'detect cavity' function of Q-site Finder (<http://www.modelling.leeds.ac.uk/qsitefinder/>). It is an energy-based method for the prediction of protein-ligand binding sites.

Sequence alignment and conserved motif prediction:

COX-1 and COX-2 from *M. musculus* were taken for sequence alignment with homologues from other organisms, viz., *Rattus norvegicus*, *Oryctolagus*, *Homo sapiens*, *Pongoabelii*, *Monodelphis domestica*, *Ornitho rhynchusanatinus*, *Anolis carolinensis*, *Xenopus tropicalis*, *Taenio pygiaguttata*, *Meleagris gallopavo*, *Gallus gallus* (Figure 3) and distribution of conserved motifs were identified by means of MEME (<http://meme.sdsc.edu>).

Docking

The binding of ligand molecule with the COX-1 and COX-2 protein molecules was performed using Docking Server (<http://www.dockingserver.com/web>) and SwissDock (<http://swissdock.vital-it.ch/>), which integrates a number of computational chemistry software specifically aimed at correctly calculating parameters needed at different steps of the docking procedure, i.e., accurate ligand geometry optimization, energy minimization, charge calculation, docking calculation and protein-ligand complex representation, and high-quality docking based on a novel optimization technique combined with a user interface experience focusing on usability and productivity. Its advanced visualization and analysis examined ligand-receptor interactions and finely tuned the docking solutions. Docking calculation, coordination and interaction were done using Discovery Studio 3.1.

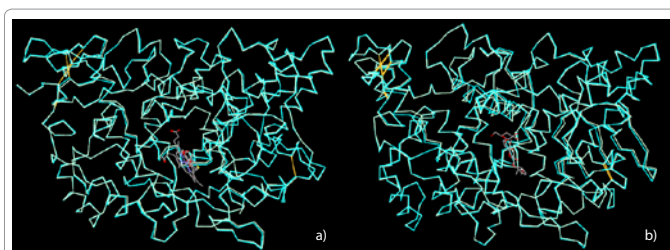


Figure 2: Superimposition of docked model with crystal structures for (a) COX1 (1PTH) structure with HEME (protoporphyrin ix containing FE) ligand and (b) COX2 (1CVU) structure with BOG (b-octylglucoside) ligand.

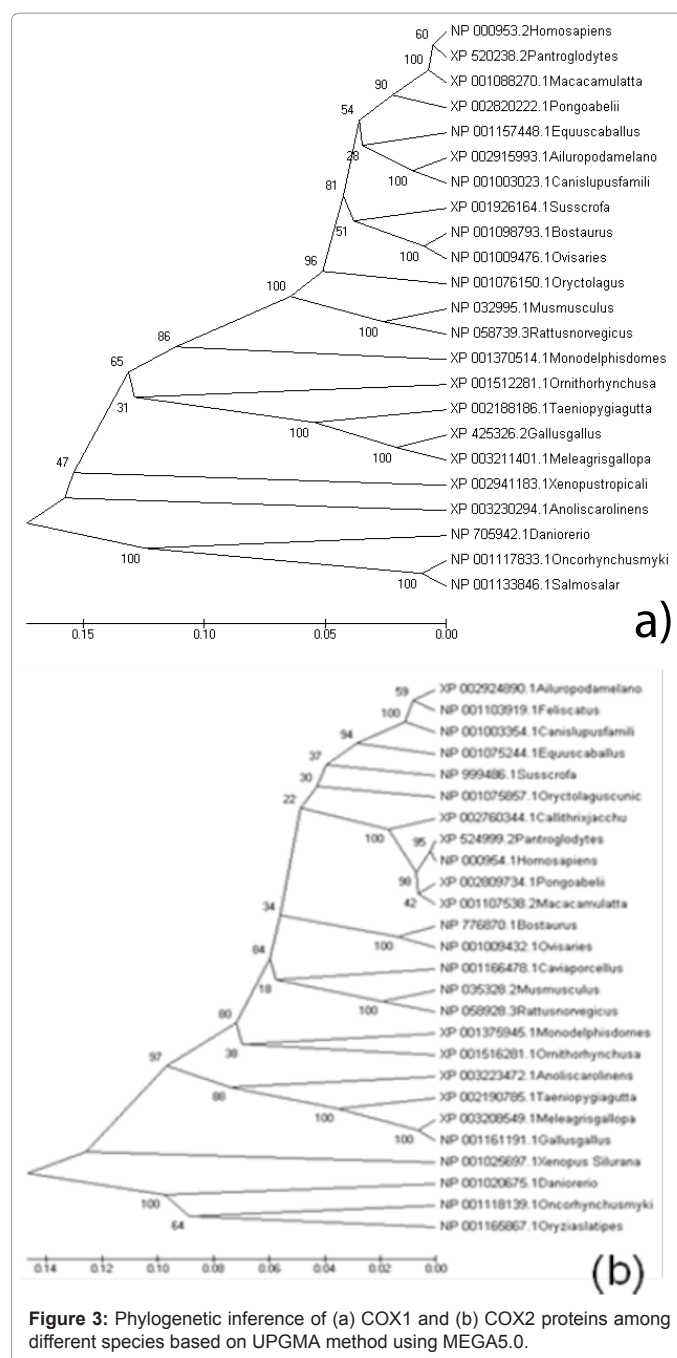


Figure 3: Phylogenetic inference of (a) COX1 and (b) COX2 proteins among different species based on UPGMA method using MEGA5.0.

www.dockingserver.com/web) and SwissDock (<http://swissdock.vital-it.ch/>), which integrates a number of computational chemistry software specifically aimed at correctly calculating parameters needed at different steps of the docking procedure, i.e., accurate ligand geometry optimization, energy minimization, charge calculation, docking calculation and protein-ligand complex representation, and high-quality docking based on a novel optimization technique combined with a user interface experience focusing on usability and productivity. Its advanced visualization and analysis examined ligand-receptor interactions and finely tuned the docking solutions. Docking calculation, coordination and interaction were done using Discovery Studio 3.1.

Transplantation of tumor

EAC cells were obtained from National Centre for Cell Sciences (NCCS), Pune, India. The EAC cells were maintained *in vivo* in female Swiss albino mice (22-25 g) by intraperitoneal transplantation of 2×10^6 cells per mouse after every 10 days. Ascitic fluid was drawn out from EAC tumor bearing mice at the log phase (days 7-8 of tumor bearing) of the tumor cells. Each animal received 0.1 ml of tumor cell suspension containing 2×10^6 tumor cells intraperitoneally.

Treatment schedule

Swiss albino mice were divided into 5 groups (n=20) and were injected with EAC cells (2×10^6 cells/mouse) intraperitoneally except for the normal group. This was taken as day zero. On the first day normal saline (0.85%, w/v, NaCl) 5 ml/kg/mouse/day i.p. served as Group-I and EAC control (without any treatment) served as Group-II. salicin at 100 mg/kg body weight/day in Group-III and at 200 mg/kg/day in group IV, and the standard drug 5-Fluorouracil (5-FU) at 20 mg/kg/day was injected in Group-V. After twenty-four hours from the last dose and 18 h of fasting, 10 animals of each group were sacrificed by cervical dislocation to measure antitumor and hematological parameters. The rest of the animals of each group were maintained to assess their lifespan, and they were provided food and water *ad libitum*. The effect of isolated and characterized salicin on tumor growth and host's survival time were examined by studying the parameters like tumor volume, tumor cell count, mean survival time, increase in lifespan of EAC bearing mice.

Antitumor and hematological parameters

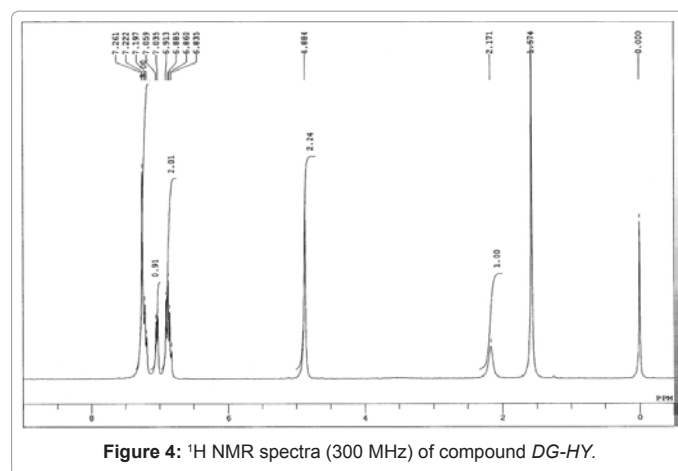
At the end of the experimental period, the next day after an overnight fasting blood was collected from freely flowing tail vein and from eye and used for the estimation of hemoglobin (Hb) content, red blood cell (RBC) count and white blood cell (WBC) count and differential count of WBC. Along with ascitic fluid was collected from the peritoneal cavity for tumor volume, tumor weight, percentage increase in life span, tumor cell count, viable/nonviable tumor were measured.

Results

Cancer is one of the life-threatening diseases, and identification of active drug targets against proteins involved in cancer like COX is of great interest. Medicinal compounds like Salicin have anti-inflammatory activity, due to which they may serve as an active drug target against many toxic/pathogenic proteins like COX-2 in our study. Interaction of COX proteins with drugs like aspirin and ibuprofen shows pharmacological inhibition of this protein and thus relieve many symptoms of inflammation and pain. Salicin is found to be as active drug target in our study as it shows inhibition of COX-1 and particularly COX-2, indicated that it may be useful in chemoprevention of some cancers like colorectal cancer. The detailed results are discussed here.

Isolation and identification of salicin

Leaf extracts of *D. gangeticum* showed the active compounds. The sapogenin (DG-HY), obtained after hydrolysis of compound DG-1 was crystallized from CH_2Cl_2 -EtOH to yield white plates (10 mg, m.p. 83-85°C). In 300 MHz ^1H NMR spectrum recorded in CDCl_3 (Figure 4), the sapogenin (DG-HY) exhibited four aromatic proton resonance signals. A 1, 2-disubstituted benzene ring was evident from the signals observed at δ 7.05 (1H, d, J=7.5) for H-3, 7.22 (1H, m) for H-5, 6.91 (1H, m) for H-4 and 6.86 (1H, d, J=7.5) for H-6. Signal characteristic to



phenolic hydroxyl group was observed at δ 7.19, while a broad singlet for aliphatic hydroxyl group at δ 2.17 and a methylene singlet at δ 4.88 evidenced the presence of hydroxyl methyl side chain in the sapogenin DG-HY.

The 75 MHz ^{13}C NMR spectrum (Figure 5) of DG-HY recorded in CDCl_3 showed a total of seven carbon resonance signals i.e. ($>\text{C} \times 2$, $>\text{CH} \times 4$, $>\text{CH}_2 \times 1$). The two carbon resonances at δ 155.9 and δ 124.6 were assigned for C-1 and C-2, respectively. The signal for hydroxyl methylene resonance was observed at δ 64.5, while the signals at δ 127.8, δ 120.0, δ 129.4 and δ 116.4 were identified for tertiary carbons C-3, C-4, C-5 and C-6, respectively.

Finally, the compound DG-1 was identified as 2-(hydroxymethyl) phenyl hexopyranoside, also known as 'salicin', on the basis of comparison of physical (melting point and elemental analysis) and spectroscopic data (UV, IR, ^1H NMR, ^{13}C NMR and mass spectra) to literature reports [52-55]. In the absence of an authentic sample, a direct comparison was not possible. This is the first report of isolation of salicin, from leaves of *D. gangeticum*.

Ligand properties computed from structure

Salicin ($\text{C}_{15}\text{H}_{18}\text{O}_7$) (Figure 6) has molecular weight of 286.27782 [g/mol], having 5 donor and 7 acceptor H-bonds. The monoisotopic mass is 286.105253. The table 1 described all the properties of Salicin compound. IUPAC Name of this compound (2R,3S,4S,5R,6S)-2-(hydroxymethyl)-6-[2-(hydroxymethyl)phenoxy]oxane-3,4,5-triol with Canonical SMILES: C1=CC=C(C(=C1)CO)OC2C(C(C(C(O2)CO)O)O)O and Isomeric SMILES: C1=CC=C(C(=C1)CO)O[C@H]2[C@H]([C@H]([C@H]([C@H](O2)CO)O)O)O. Retrieved Chemical compound (CID_439503) total MMFF94 energy was 62.975 and shape volume was 207.7 obtained from Discovery Studio 3.1. To evaluate better drug likeness within the limits proposed by Lipinski's rule of five, salicin compound have follows molecular weight, number of hydrogen donor and acceptors bonds according to rule.

Model Details

Homology modeling

The three dimensional structures for COX-1 and COX-2 proteins were constructed using PDBID 1CQE X-ray diffraction with resolution of 3.10 Å with E-Value: 0.0 and Score 2596, Identity 84%, Positivity 89% for COX-1 and PDBID 1CVU X-ray diffraction with resolution of 2.40 Å with E-Value 0.0, Score: 2882 Identity 97%, Positivity 97%

for COX-2. Based Template 1CQE for COX-1 and 1CVU for COX-2 was used for model construction using homology modeling tool DS MODELER (Figure 7). The Predicted 2D and 3D structures provide valuable insight into functional regulatory region in secondary elements and also enable the identification of possible interaction site for a suitable inhibitor. Among the three conformations generated the one with the least modeller objective function value was considered to be thermodynamically stable and was chosen for further refinement and validation.

Based on the structural alignment of the amino acid sequences of the COX-1 and COX-2, a theoretical model of these proteins was obtained, corresponding with amino acid residues 34–586 for COX-1 and residues 18-569 for COX-2 of the primary structure (Figure 8).

Evaluation and refinement

The rough models for COX-1 and COX-2 were subjected to energy minimization using conjugate gradient algorithm with maximum steps 200 and RMS gradient 0.1 to eliminate bad contacts between amino acid atoms using simulation tool of Discovery Studio 3.1. The backbone conformation of the rough model was inspected using the Phi/Psi Ramchandaran plot obtained in the PDBSum server (<http://www.ebi.ac.uk/pdbsum/>). The results of Ramchandaran plot indicate that the rough model generated for COX-1 had no residue in the disallowed region whereas that for COX-2 had two residues, viz., Glu384 and Ser482, in the disallowed region, occurring in the

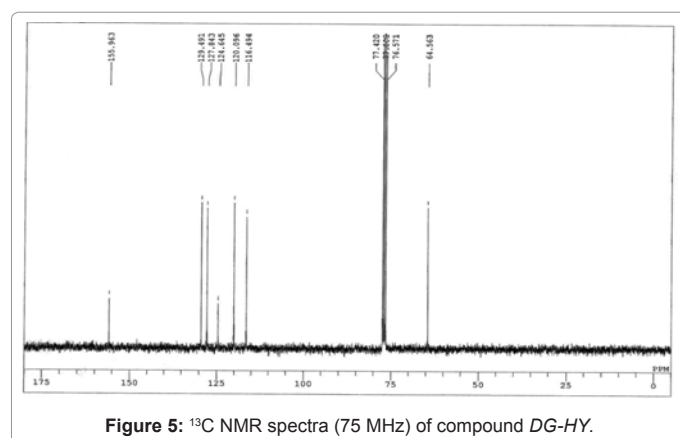


Figure 5: ¹³C NMR spectra (75 MHz) of compound DG-HY.

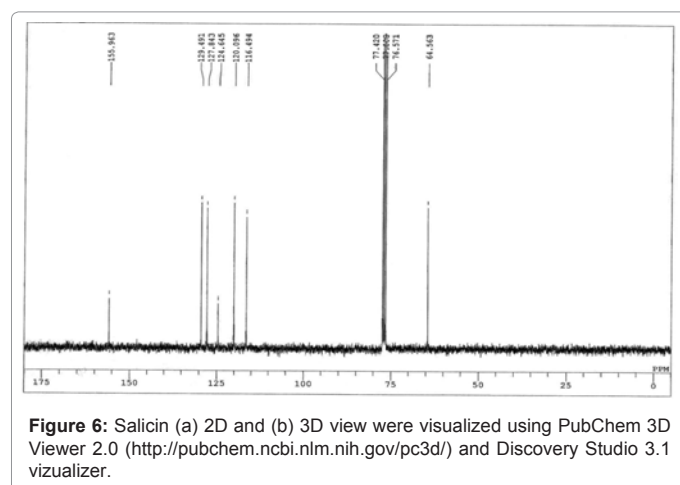


Figure 6: Salicin (a) 2D and (b) 3D view were visualized using PubChem 3D Viewer 2.0 (<http://pubchem.ncbi.nlm.nih.gov/pc3d/>) and Discovery Studio 3.1 vizualizer.

Characteristics	Properties
Molecular weight	286.27782 [g/mol]
Molecular formula	C ₁₃ H ₁₈ O ₇
H-bond donor	5
H-bond acceptor	7
Exact mass	286.105253
Monoisotopic mass	286.105253
Topological polar surface area	120
Covalently-bonded unit count	1
Feature 3D acceptor count	7
Feature 3D donor count	5
Feature 3D ring count	2
Effective rotor count	5.2
Conformer sampling RMSD	0.8

Table 1: Ligand properties of salicin for drug targeting.

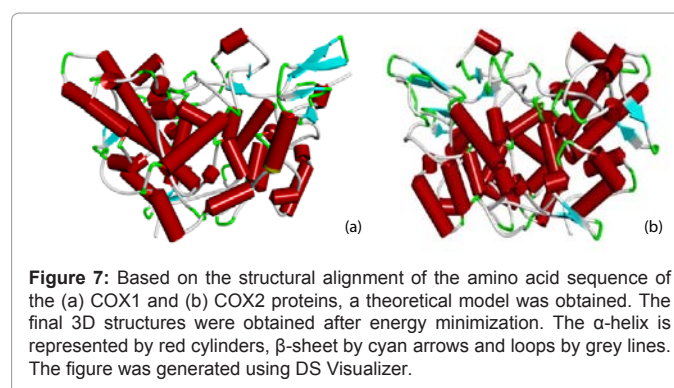


Figure 7: Based on the structural alignment of the amino acid sequence of the (a) COX1 and (b) COX2 proteins, a theoretical model was obtained. The final 3D structures were obtained after energy minimization. The α -helix is represented by red cylinders, β -sheet by cyan arrows and loops by grey lines. The figure was generated using DS Visualizer.

loop. Loop refinement was done using looper and CHARMM based molecular mechanics to generate multiple energy optimized variants of the selected segments of the protein structure. Side chain refinement was done using chi-rotator, a CHARMM based energy minimization, a routine tool to optimize the conformation of the selected amino acid side chain atoms (Table 2).

The Ramchandaran plot statistics showed that 89.9% residues were in the most favored regions with Φ and Ψ angles in the core of favored regions and 10.1% of residues were in additional allowed regions for COX-1, while for COX-2 90.7% residues were in the most favored regions and 9.3% of the residues occurred in additional allowed regions (Figure 9). This result was also verified by RAMPAGE server (<http://mordred.bioc.cam.ac.uk/~rapper/rampage.php>). There are no residues either in the generously allowed region and or in disallowed region in COX-1 and COX-2 had two residues, viz., Glu384 and Ser482, in the disallowed region, after evaluation and refinement.

Model quality estimation

ProSA-web server (<https://prosa.services.came.sbg.ac.at/prosa.php>) shows overall model quality by comparing the potential of mean forces derived from a large set of known NMR and X-ray deciphered structures of similar sizes and group. The model quality assessment is graphically presented in form of Z score; in our study Z scores were found to be -8.86 and -9.23 for COX-1 and COX-2 respectively,

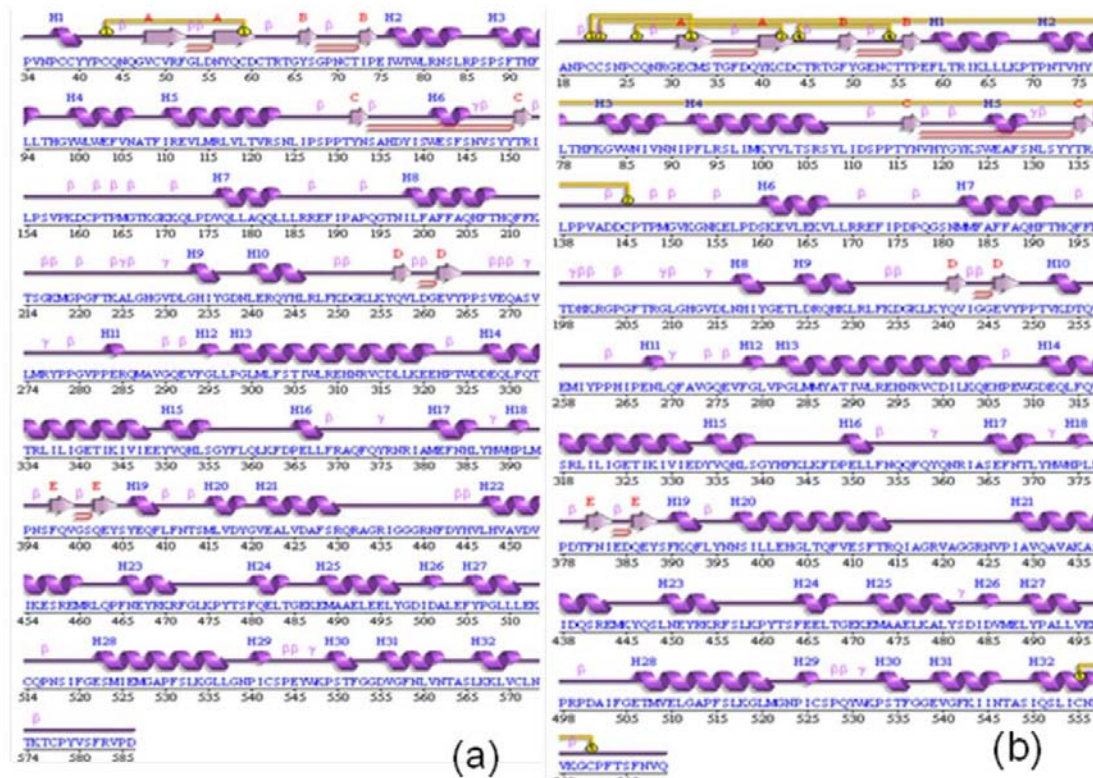


Figure 8: The two dimensional structure annotation of (a) COX1 and (b) COX2 protein molecules from *M. musculus*. The α -helices, β -sheets and coils are indicated in the figure generated using PDBSum.

Before energy minimization for COX-1 (Kcal/mol)	After energy minimization for COX-1 (Kcal/mol)	Before energy minimization for COX-2 (Kcal/mol)	After energy minimization for COX-2 (Kcal/mol)
-15095.82367	-34857.28680	-19369.215661	-35925.71513

Table 2: Discovery Studio energy values for COX-1 and COX-2 proteins.

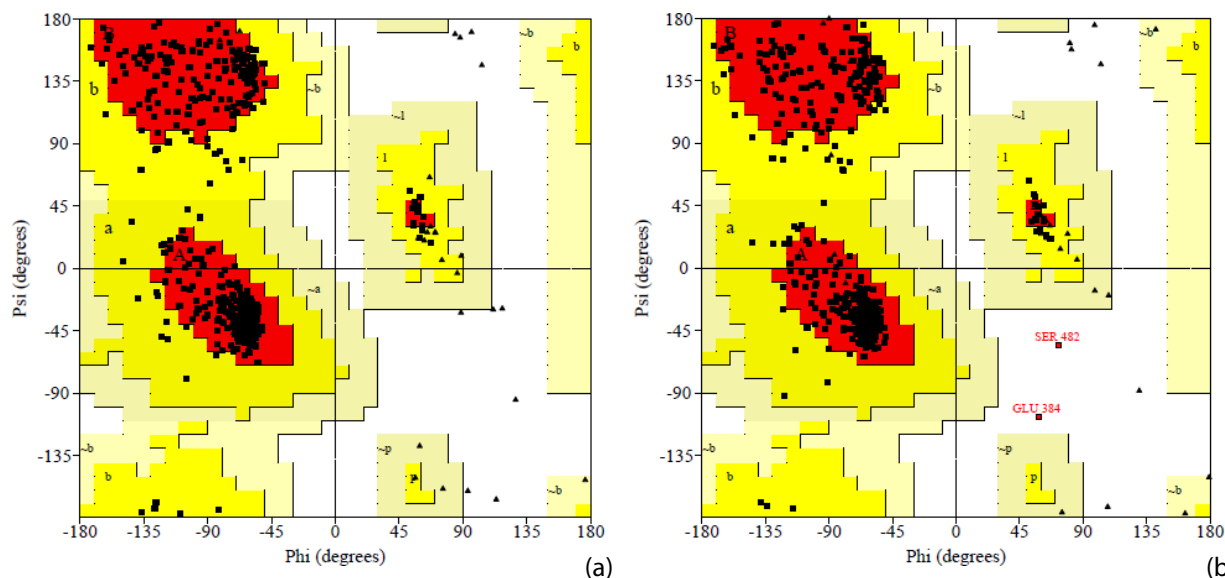


Figure 9: Ramachandran plots of COX1 and COX2 proteins built using Discovery Studio 3.1 software. The plot calculations on the 3D model of COX proteins were computed with the PROCHECK server.

suggesting the model being within the permissible range of native conformational structures.

QMEAN server (<http://swissmodel.expasy.org/qmean/cgi/index.cgi>), model quality estimation, was used to analyze QMEAN score, residue error, energy profiles and plot and volume area dihedral angle for fractional accessible surface area, residue volume, 3D profile and stereo/packing quality index were done with VADAR (<http://vadar.wishartlab.com/>). QMEAN and VADAR were specially designed for quantitative and qualitative assessment of protein structures determined by X-ray crystallography, NMR spectroscopy, 3D-threading or Homology modeling. QMEAN score of the whole model reflecting the predicted model reliability range from 0 to 1. In this study, the predicted COX-1 model QMEAN score was 0.654 with global scores estimated absolute quality Z-score of -1.32; these results show that the model is reliable. Fractional accessible surface area volumes of all residues close to 1.0 ± 0.1 , statistics of hydrogen bonds of predicted model show equal to expected mean H bond distance score of $2.2 \text{ sd}=0.4$ equal to the expected value, Mean H bond energy observed $-1.7 \text{ sd}=1.1$ close to the expected $-2.0 \text{ sd}=0.8$. Dihedral Angles were observed close to the expected, Total Accessible Surface Area score $23870.3 \text{ Angs}^{**2}$ with expected score $20013.5 \text{ Angs}^{**2}$, Total volume (packing) score observed $85910.2 \text{ Angs}^{**3}$ with expected $77534.2 \text{ Angs}^{**3}$, Stereo/Packing, 3D quality index results show no error residues in the predicted model. In this predicted COX-2 model QMEAN score 0.603 with global scores estimated absolute quality Z-score of -1.94 indicate that the model is reliable. Fractional accessible surface area volumes of all residues is close to 1.0 ± 0.1 , statistics of hydrogen bonds of predicted model is equal to the expected mean H bond distance score of $2.2 \text{ sd}=0.4$, Mean H bond energy observed was $-1.7 \text{ sd}=1.1$ that is close to the expected $-2.0 \text{ sd}=0.8$. Dihedral Angles were observed to be close to the expected, Total Accessible Surface Area score was $23652.7 \text{ Angs}^{**2}$ with expected score of $19948.1 \text{ Angs}^{**2}$, Total volume (packing) score was observed $83467.8 \text{ Angs}^{**3}$ with expected of $77179.1 \text{ Angs}^{**3}$, Stereo/Packing, 3D quality index results shows that no error residues occur in the predicted model. After complete reliability test based on quantitative and qualitative assessment, the predicted Models of COX-1 and COX-2 from *M. musculus* were deposited in Protein Model Database (PMDb) with PMDBID PM0077492 (http://mi.caspar.it/PMDB/user/model_info.php?id=77492) and PM0077493 (http://mi.caspar.it/PMDB/user/model_info.php?id=77493), respectively.

Superimposition of the 3D predicted model with template were done with Combinatorial Extension (CE) Method based server (<http://cl.sdsc.edu/>). The superimposed backbone traces displayed Z-Score=8.4 and Rmsd=0.3 Å with sequence identity=89.5% for COX-1, while for COX-2 Z-Score=8.4 and Rmsd=0.4 Å with sequence identity=99.5% for all atoms calculated locally within the two polypeptide chains (Figure 2). Most bond lengths, bond angles, and torsion angles were between values expected for a naturally folded protein.

Active site residue details

Among the ten sites obtained from Q-site finder, only 3 sites were selected, since they were conserved among different species, and the other sites are not further discussed. In both the proteins, site 2 is highly conserved in the active sites of the template and predicted COX-1 and COX-2 models (Figure 10). Results from multiple sequence alignment and Motif analysis revealed that at COX-1 site 2, Tyr150, Ala201, Phe202, Ala204, Gln205, Thr208, His209, Phe212, Lys 213, Thr214, Leu296, Tyr350, Asn384, Tyr387, His388, Trp389, His390, Leu392, Met393, Phe397, Tyr406, Phe409, Leu410 and Val446 residues

are conserved, and at the COX-2 site 2, Tyr 134, Thr192, His193, Phe196, Lys197, Thr198, Asp199, His200, Lys201, Arg208, Asn217, His 218, Gly221, Glu222, Thr223, Arg226, Gly274, Gln275, Glu276, Val277, Asn368, His372 are conserved (Table 3). Sequence analysis of the proteins depicts low substitution rate and less gap penalty, which indicates that they belong to the same protein family. Thus, site 2 of both COX-1 and COX-2 proteins has been found to be the most favorable site for docking studies. Motifs obtained from MEME tool, 29 for COX-1 and 21 for COX-2 out of selected maximum number of 30 motifs with length 20 to 50 (Figure 11). In which motif 2 and motif 5 represent the functional motif for both COX proteins containing the active site residues and catalytic residues, which are highly conserved and most representative among different species (Figure 12). The sequences which are highly representative and conserved throughout evolutionary studies are marked by red box in figure 11 (FAFFA in COX-1 and QHFTHQ and FFA in COX-2).

Docking study of COX-1 and COX-2 receptors with salicin inhibitor

Docking of COX-1 and COX-2 was performed with salicin inhibitor (2-(hydroxymethyl) phenyl hexopyranoside). The final docked conformation obtained for salicin was evaluated based on the number of hydrogen bonds formed and bond distances between atomic coordinates of the active site and inhibitor. To evaluate the structural similarity of *M. musculus* COX-1 and COX-2 with related COX proteins of different species, multiple sequence alignment (22 species for COX-1 and 25 for COX-2) was performed by UPGMA. The UPGMA (Unweighted Pair Group Method with Arithmetic Mean) phylogenetic profile based on reliability of an inferred tree is based on Felsenstein's [56] bootstrap test, which is evaluated using Efron's [57] bootstrap resampling technique (Figure 3). It was observed that the following stretch Ala201-Phe202-Ala204-Gln205, Thr208-His209, Phe212-Lys213-Thr214, Tyr387-His388-Trp389-His390, Leu392-Met 393 for COX-1 and Ala188-Gln189, Thr192- His193, Phe196, Asn368, Tyr371-His372, His374, Leu377 for COX-2 were conserved and present in catalytic active residues. Among these stretches the Thr208, Tyr387 and Trp389 amino acids residues may be involved in hydrogen bond interaction with salicin in the case of COX-1, while in case of COX-2 Ala 188, Gln189, Thr192, His193, Phe196, Asn368, Tyr371, His372, His374, Leu377 amino acid residues appear to be involved. Based on docking of COX proteins with salicin inhibitor COX-2 having more hydrogen bond with greater affinity interaction rather than COX-1. The hydrogen bond interactions between inhibitor and COX proteins along with the bond distances are shown in table 4 and figure 13.

Effect of salicin on tumor volume and survival time

There were no gross behavioral changes and mortality upto a dose level of 200 mg/kg body weight. The LD50 value of salicin compound was found to be $> 2 \text{ g/kg}$ body weight of mice indicating that it has low toxicity to the animal. Treatment with salicin at the dose of 100 and 200 mg/kg body weight increased the lifespan (ILS) and nonviable cell count and significantly reduced the tumor volume, tumor weight and viable tumor cell count when compared to that of EAC control group (Table 5).

The effect of salicin on hematological studies

The haemoglobin content, RBC count, lymphocyte (%) and monocyte (%) in EAC bearing mice given salicin at the dose of 100 and 200 mg/kg increased significantly compared with those in EAC control, whereas WBC count and neutrophil (%) showed significant

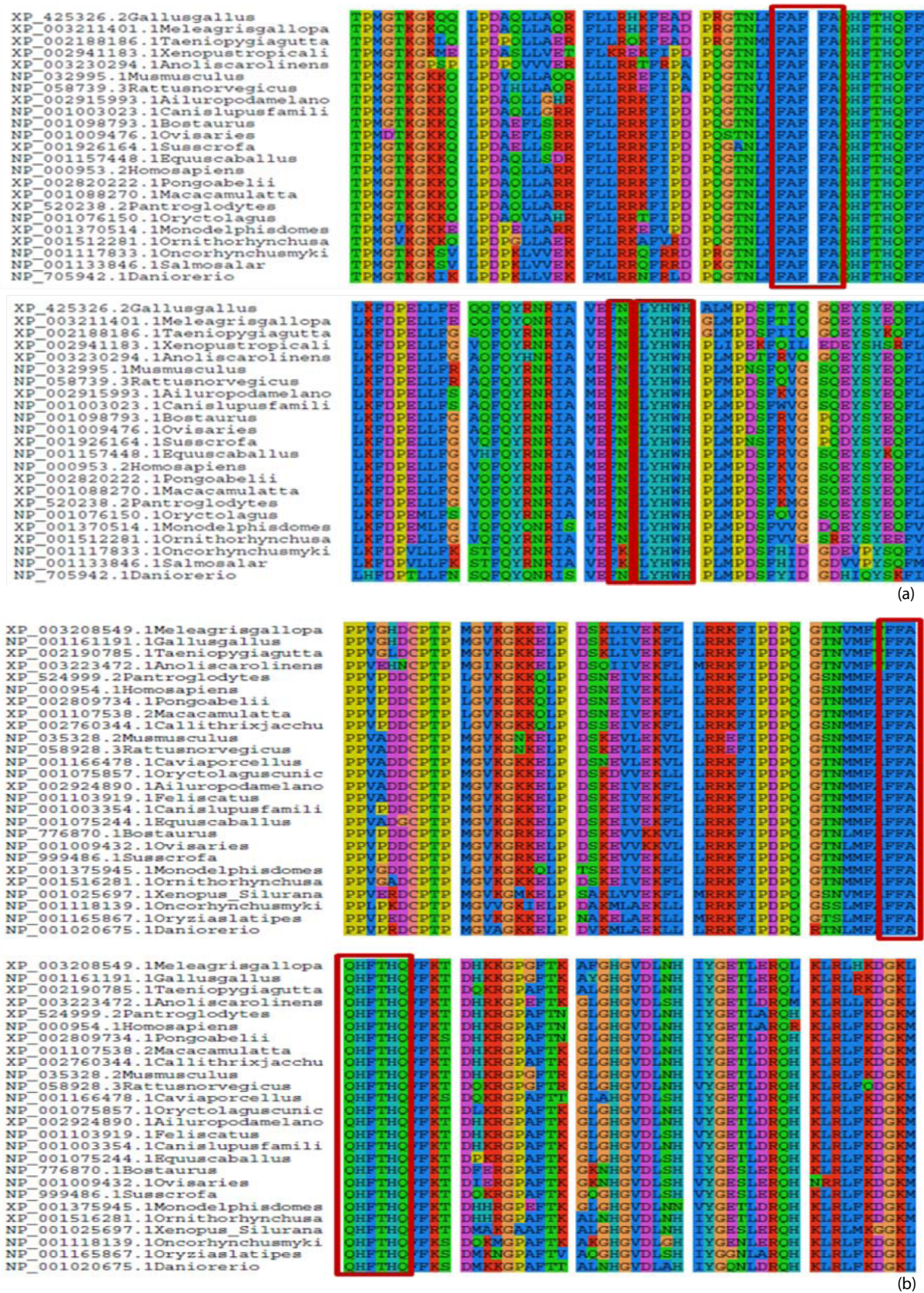


Figure 10: Multiple sequence alignment of COX proteins from different species, the conserved residues across various species are boxed in red.

Citation: Srivastava P, Singh VK, Singh BD, Srivastava G, Misra BB, et al. (2013) Screening and Identification of Salicin Compound from *Desmodium gangeticum* and its *In vivo* Anticancer Activity and Docking Studies with Cyclooxygenase (COX) Proteins from *Mus musculus*. J Proteomics Bioinform 6: 109-124. doi:10.4172/jpb.1000269

COX-1			COX-2		
Site 1	Site 2	Site 3	Site 1	Site 2	Site 3
ASN 36	TYR 150	VAL 118	ASN 19	TYR 134	ALA 185
CYS 38	ALA 201	ARG 122	CYS 22	THR 192	PHE 186
CYS 39	PHE 202	TYR 350	SER 23	HIS 193	ALA 188
TYR 41	ALA 204	VAL 351	ASN 24	PHE 196	GLN 189
PRO 42	GLN 205	LEU 354	PRO 25	LYS 197	THR 192
CYS 43	THR 208	SER 355	CYS 26	THR 198	HIS 193
GLN 44	HIS 209	TYR 357	GLN 27	ASP 199	PHE 196
ASN 45	PHE 212	LEU 361	ASN 28	HIS 200	ASN 368
GLN 46	LYS 213	PHE 383	ARG 29	LYS 201	TYR 371
GLY 47	THR 214	LEU 386	GLY 30	ARG 208	HIS 372
VAL 48	LEU 296	TYR 387	GLU 31	ASN 217	TRP 373
CYS 49	TYR 350	TRP 389	CYS 32	HIS 218	HIS 374
VAL 50	ASN 384	PHE 520	MET 33	GLY 221	LEU 377
ARG 63	TYR 387	MET 524	SER 34	GLU 222	
THR 64	HIS 388	ILE 525	ASP 111	THR 223	
TYR 66	TRP 389	GLY 528	THR 115	ARG 226	
ARG 81	HIS 390	ALA 529	TYR 116	GLY 274	
LEU 125	LEU 392	SER 532	GLY 121	GLN 275	
PRO 127	MET 393	LEU 533	TYR 122	GLU 276	
THR 131	PHE 397		LYS 123	VAL 277	
TYR 132	TYR 406		ALA 137	ASN 368	
ASP 137	PHE 409		LEU 138	HIS 372	
TYR 138	LEU 410		PRO 140		
ILE 139	VAL 446		VAL 141		
ILE 153			ALA 142		
LEU 154			CYS 145		
PRO 155			MET 149		
SER 156			GLY 150		
VAL 157			GLN 447		
PRO 158			GLU 451		
LYS 159			TYR 452		
GLN 463			LYS 454		
GLU 467			ARG 455		
LYS 470			SER 457		
ARG 471					
PHE 472					
GLY 473					

Table 3: 3 best predicted active sites for COX1 and COX2 from 10 predicted sites obtained from Qsite Finder <http://www.modelling.leeds.ac.uk/qsitefinder/>.

Motif	Width	Best possible match	Motif	Width	Best possible match
1	50	DIDALEFYPLLEKCHNSIFGESMIEIGAPFSLKGLLGNPICSPYEWK	1	50	MMYATIWLREHNRVCDVLKQEHPEUDDQLFQTSRLILIGETIKIVIEDY
2	50	QGTNLMFAFFAQFTHQFFKTSQKMGPOFTKALGHGVDLGHLYGDNLERQ	2	50	VQLLSGYHFKLKFPELLFNQQFQYQNRIAAEFNTLYHWHPLLPTFFQIH
3	50	NPCCYYPCQHQICVRFGLDRYQCDCTRTGYSQPNCTIPELWTLRNSLR	3	50	GAPFSLKGLMGNFICSPEYWKSTFGGEVGFKIINTASIQSLICMNVKGC
4	50	SNLIPSPPTYSADHYISWESYNSVSYTRILPSVFKDCPTPMGTGKQKQ	4	50	YVLTSRSLIDSPTYNADYGYKSWAEAFMSLSYTRALPPVDDCPTMG
5	50	QFQYRMRAMEFNQLYWHPLMPSFKVGSQESYEQFLFNTSMLVYGV	5	50	RKFLPDPOGTMFAFFAQFTHQFFKTDKRGPAFTKGLGHGVDLNHIY
6	50	NIDHVLVAVDVVKESEMRQLQFNEYRKRFGMKPYTSFOELTGEKEMA	6	50	SRQMKYQSLNEYRKRFLMKPYESFEELTGEKEMAAEALYGDIDAMELY
7	42	CDILKAHEPTUGDEQLQFTARLILIGETIKIVIEEVQQLSG	7	50	FDQYKDCCTRIGFYGENCTTPEFLTWIKLFLKPTNTVHYILTFRGVVM
8	50	YPPSVEEAPVIMDYPRGIPQSQMAVQGEVFGLLPGLMMYATIWLREHNR	8	50	KDKMKYQMDIGEMYPTVKTQVEMLYPPHVEHLRFVAGQEVFGLVPG
9	36	STFGGEMGFNIVKATLKKLVCLNTRKCPVYSFRVP	9	50	QQFIYNNISILLEHGLTQFVESFSRQIAGRVAAGRRVFAAVQKVKASIDQ
10	28	LTHGRWFUDFINATFIRDMLRVLVTVR	10	38	SVQDPQLTKVTINASSSSGLDDINPTVLLKERSTEL
11	20	YQLRLFKDCKLKYQVVDGEM	11	20	AANPCSNPCQNRGVCHSVG
12	20	PDAQLLARRFLRRKFIPTDP	12	20	FALLVEKPRDAIFGETHVE
13	28	LULWFLLLLLLPPFVLPADPGAPV	13	20	VKGGKLPDSKEIVEKFLLR
14	28	MRECVVWVACILLQRLPTCRGEEGKDA	14	20	WLSEPGRRRRRGRQDWRRKR
15	28	STFGGETGFNIVKATFROLVCRNVKQC	15	20	TMAAPGEGIPCAGGGQGRW
16	20	DAVAAGETDSGRVGGASSPE	16	24	WVRARDEPRNTICNINTHQGVW
17	20	TAPLGYSKVKAAPRVGD	17	20	MMKRISRLLFFSGIIFVQC
18	28	MSREFDPDAPGNPLCLPGEPRMPPGDLT	18	20	DALRQQGNPPRRRPPCAMK
19	20	FNALKRWEDQPCGAYAGN	19	20	MNSMRARPSLRDFSDCEG
20	20	DSDICGHVPGFLGCVVIVA	20	20	MNSVRAVSRNSAAGPPVCEG
21	22	MRECDFAKGGIFLASGGAFCA	21	20	MRCRRVFCPPVGHPRCEG
22	20	CCMAGQGVFGFCFCQAVRR			
23	20	CTRPPQCPPIAPFCAGAGCV			
24	20	QRGEUGRDMLMCMFVGLV			
25	20	FFVAFVQVDDVLEKEDK			
26	20	RVGREGRPREEMGRANGEM			
27	20	TKISPGRCPEENEKPIFACS			
28	20	VPVGFVRGSGSYDTEVGDV			
29	20	MPPKEEGSGPQVYPRGIRR			

Figure 11: Multilevel consensus sequences for the MEME defined motifs observed among different COX proteins from *M. musculus*.

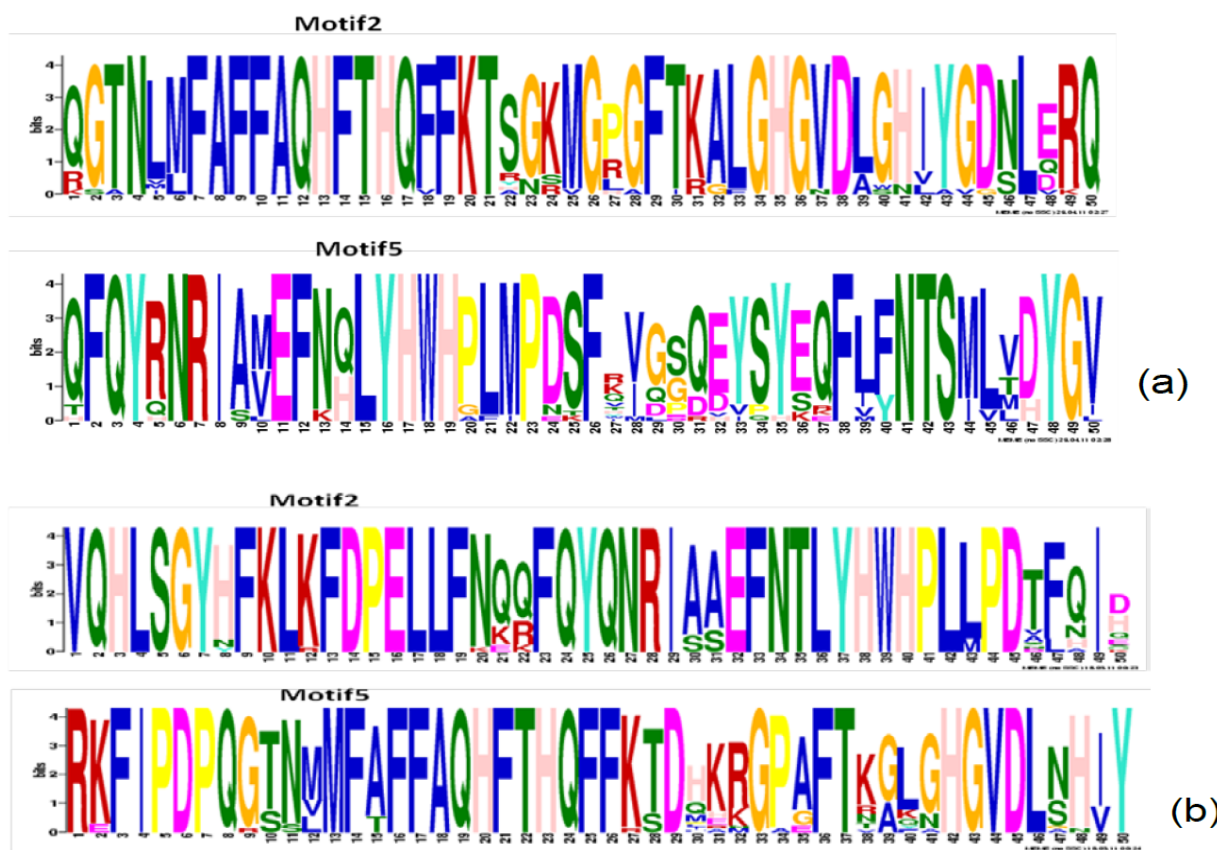


Figure 12: Highly represented sequence LOGO obtained from MEME/MAST server (http://meme.sdsc.edu/meme4_6_1/cgi-bin/mast.cgi).

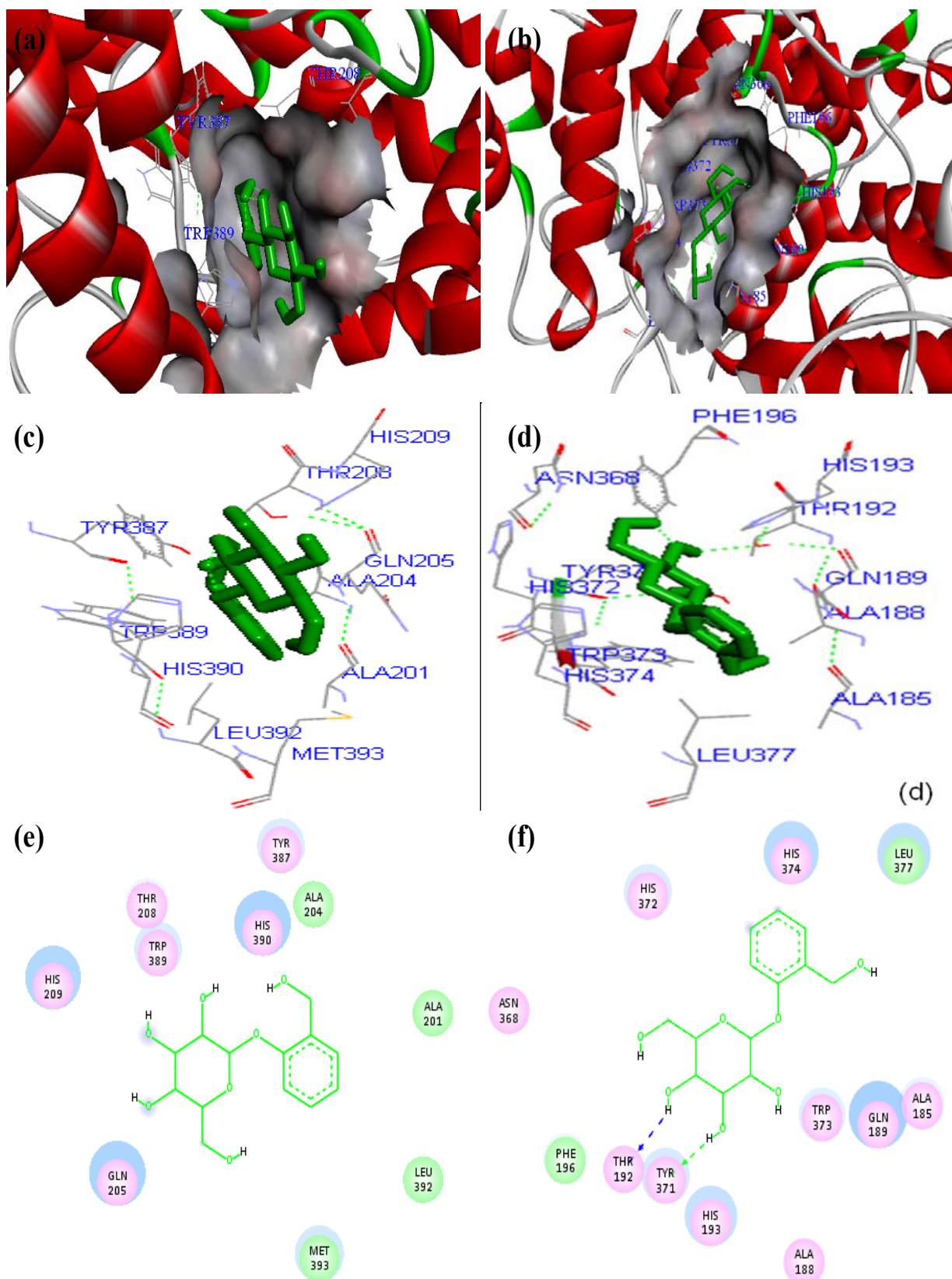


Figure 13: COX protein complex with salicin inhibitor. Surface view of (a) COX1 and (b) COX2, hydrogen bond interactions of (c) COX1 and (d) COX2, Overall bond interactions (e) COX1 and (f) COX2 using DS modeling vizualizer 3.1.

decrease (Table 6). Treatment with salicin restored the hematological parameters to more or less normal values. The number of RBC count and hemoglobin content also increased, while the WBC and the differential count decreased as compared to that of EAC control. Treatment with salicin illustrated the percent increase in tumor cell volume and numbers of viable tumor cells were found to be significantly less when compared to those of the EAC control. Hence, it can be concluded that the extracts by their cytotoxic effect and arresting the tumor growth, increased the life span of EAC bearing mice. The percentage increase in life span in response to the 200 mg/kg body weight of salicin administration was indicating its potent anticancer nature (Table 6). In

acute toxicity studies, the administration of salicin at the dose of 100 mg/kg and 200 mg/kg for 14 days did not exhibit any adverse effect.

Discussion

In the early 1990s, cyclooxygenase (COX) was demonstrated to exist as two distinct isoforms. COX-1 is constitutively expressed as a housekeeping enzyme in nearly all tissues, and mediates physiological response, e.g., cytoprotection of the stomach, platelet aggregation. COX-2, on the other hand, is expressed by cells that are involved in inflammation, e.g., macrophages, monocytes, synoviocytes, and has emerged as the isoform that is primarily responsible for synthesis of

COX-1				COX-2			
Residue	Atom	Salicin	Distance Å	Residue	Atom	Salicin	Distance Å
ALA 204	CB	C10	3.45	ALA 188	CB	H3	3.17
GLN 205	OE1	O1	3.67	GLN 189	CB	H3	3.74
THR 208	OG1	H3	3.87	THR 192	OG1	H2	2.12
HIS 209	NE2	H1	3.60	HIS 193	CE1	O6	3.79
TYR 387	CD1	C11	3.90	PHE 196	CD2	H4	3.67
TRP 389	CB	C8	3.75	ASN 368	ND2	H4	3.89
HIS 390	CD2	H4	3.73	TYR 371	CB	H2	3.85
LEU 392	CD1	C13	3.16	HIS 372	O6	NE2	3.49
MET 393	CE	C12	3.37	HIS 374	CD2	C7	3.38
				LEU 377	CD1	C13	3.68

Table 4: Hydrogen bonds along with their distances between the salicin inhibitor and active site residues of COX proteins as deciphered using Docking server.

Parameters	EAC control	100 mg/kg salicin	200 mg/kg salicin	5-FU
Tumor volume (ml)	3.15 ^a	1.68 ^c	0.99 ^e	0.47 ^f
Tumor weight (g)	3.81 ^a	1.52 ^b	0.89 ^c	0.42 ^f
MST (days)	22	34	40	43
%ILS	0.0	54.54	81.81	95.45
Viable cell count	7.9×10 ^{7a}	3.1×10 ^{7b}	1.3×10 ^{7d}	0.9×10 ^{7e}
Nonviable cell count	0.8×10 ^{7e}	1.9×10 ^{7d}	2.8×10 ^{7b}	3.4×10 ^{7a}
Total cell count	8.4×10 ⁷	5.0 ×10 ⁷	4.1×10 ⁷	4.3×10 ⁷

Each point represents the mean (n=10 mice per groups).

*The values marked with the different letters show significant difference (Duncan's multiple range test, P<0.05).

Table 5: Effect of the isolated salicin compound from leaves of *D. gangeticum* on tumor volume, tumor weight, mean survival time (MST), percentage increase life span (%ILS), viable and nonviable, tumor cell count in EAC bearing mice.

Parameters	Normal Saline (0.5 ml/kg)	EAC (2×10 ⁶ cells) control	EAC (2×10 ⁶ cells) + 100 mg/kg salicin	EAC (2×10 ⁶ cells) + 200 mg/kg salicin	EAC (2×10 ⁶ cells) + 5-FU
Haemoglobin content (g/dl)	13.8 ^a	11.1 ^e	12.1 ^d	12.9 ^c	13.1 ^b
Total RBC*	6.1 ^a	4.2 ^{ef}	5.0 ^d	5.7 ^{bc}	5.9 ^b
Total WBC**	8.2 ^a	14.9 ^a	11.2 ^b	9.9 ^c	9.0 ^d
Lymphocyte (%)	65.9 ^a	23.7 ^d	58.8 ^b	63.4 ^c	65.1 ^{ab}
Neutrophil (%)	32.1 ^f	73.7 ^a	38.5 ^c	33.7 ^d	32.6 ^{ef}
Monocyte (%)	3.4 ^c	2.2 ^f	3.1 ^d	3.9 ^b	4.2 ^a

* (cells/ml ×109); ** (cells/ml ×106)

Each point represents the mean (n=10 mice per groups).

The values marked with the different letters show significant difference (Duncan's multiple range test, P<0.05).

Table 6: Effect of salicin of *D. gangeticum* on hematological parameters of EAC treated mice.

the prostanoids involved in pathological processes, such as acute and chronic inflammatory states [58]. The two known COX isoforms show a high degree of similarity in their amino-acid sequences [59-62] and structural topology [63-65].

Classical NSAIDs like aspirin, ibuprofen, naproxen, but not nimesulide, are non-selective inhibitors of both the COX isozymes (IC₅₀ for COX-1 is similar to that for COX-2) and their prolonged use can cause gastric bleeding and renal failure [66-68]. Hence, there have been sustained effort to identify selective COX-2 inhibitors, i.e., compounds whose IC₅₀ for COX-1 inhibitory activity is significantly greater than that for COX-2. Some COX-2 inhibitors have been evaluated in clinical trials, but some of them showed increased cardiovascular toxicity; celecoxib, however, seems to be relatively safe COX-2 inhibitor [58]. It has meanwhile been hypothesized that there might be other isoforms of the COX enzyme yet to be discovered [67].

Nexrutine is a herbal alternative to COX inhibitor drugs for pain and soreness, and offers a number of advantages over both broad COX-1/2 inhibitors like aspirin and selective COX-2 inhibitors like Celebrex. Nexrutine inhibits the inflammatory COX-2 connected with pain without inhibiting the protective COX-1; thereby having a lower risk of producing gastrointestinal and bleeding side effects compared aspirin and Celebrex [69]. Synthetic compounds like mono-, di-, and triaryl substituted tetrahydropyrans were also reported as COX-2 and tumor growth inhibitors. These compounds exhibit IC₅₀ for COX-2 in the range 0.57-4.0 nM, and their selectivity for COX-2 over COX-1 is better than that of celecoxib and rofecoxib [70].

A number of docking procedures based on different search and scoring algorithms have been proposed [71], but none can treat all biological systems with the same accuracy and efficacy [72-74]. It is thus advisable once the biological target has been selected, to set up an adequate system strategy for the study goal. The bark from white willow and some legumes contain salicin which is a natural pain reliever, is very easy on the stomach and kidneys, while acetylsalicylic acid is known to upset the stomach and in some cases damage kidneys. Scientists believe that this is because salicin is converted to acetylsalicylic acid after the stomach has absorbed it [75]. Putting acetylsalicylic acid directly into the stomach damages its lining and bleeding ulcers can result. Thus salicin is a pro-drug that is gradually transported to the lower part of the intestine, hydrolysed to saligenin by intestinal bacteria, and converted to salicylic acid after absorption. It thus produces an antipyretic action without causing gastric injury [76].

COX-2 produces inflammation causing compounds that lead to swelling for curative and protection. Blocking the COX-2 enzyme completely is not good because COX-2 activity is required for cardiovascular health. Many pain killers in the past ended up blocking all COX-2 activity, which led to heart problems for the patients taking them. Today most pain killers block a part of COX-2 activity but they also block COX-1, which is vital for the health and structure of the stomach lining. The white willow bark derived pain killer does not block COX-1, but it does block COX-2; as a result, it has few reported side effects [77].

Most docking algorithms consider that the enzyme structure is rigid, according to the high computational cost induced by the flexibility of big molecules, while the ligand is free to move. Usually, in the first step, a library of ligand conformers is generated and in the second step, these conformers are docked into the target, each conformer being treated as a new ligand. Any algorithm able to generate in a correct

manner the ligand conformers could be used to generate this library. One of them is represented by genetic algorithms. Genetic algorithms attempt to use the rules of natural selection to subset computationally demanding tasks [78,79].

Qualitative and quantitative analyses of predicted 3D-structure of PMDBID PM0077492 and PM0077493 show that total Accessible Surface Area and total volume (packing) have significant reliable scores, which were compared with the experimental data available in VADAR server [80]. Secondary structure element statistics describe 44% and 46% of helices, 13% and 13% of Beta sheets, 41% and 40% of coils and 25% and 26% of turns in PM0077492 and PM0077493, respectively. After complete validation and refinement, stereochemical properties reveal no residues in the disallowed region in COX-1 and COX-2 had two residues, viz., Glu384 and Ser482, in the disallowed region. A good quality model would be expected to have over 90% residues in the most favored regions. In this study PMDBID PM0077492 and PM0077493 contain 89.9% and 90.7% residues in the most favored regions with overall average G-factor value of 0.14 and 0.17, respectively, indicating that the model quality is good.

Evolutionary sequence conservation and protein 3D structures have commonly been used to identify functionally important sites. The identification of a good catalytic active binding site and drug-protein interaction leads to identification of the potential drug target for functional inhibitory activity. The conserved active binding residues proved to be functionally enriched. Therefore multiple sequence alignment and regulatory motif detection were done to measure catalytic active binding sites with evolutionary conservation to get evidence for the best fit of a characterized salicin inhibitor. Multiple sequence alignment of COX-1 and COX-2 of *M. musculus* with different homologous species were performed (22 species for COX-1 and 25 for COX-2). The evolutionary tree was drawn using UPGMA, which suggests that *M. musculus* is closely related to *Rattus norvegicus*. This sequence analysis shows a high degree of evolutionary conservation among the active binding site within sequences of target proteins as well as in highly represented motifs. In both the COX proteins the predicted motifs were found to be conserved and most representative in sequence logo form (Figure 12). Moti10-LMRLVLTVR, Motif 2 - FAFFAQHFTHQFFKT, Motif 7 - IE[ED]YVQ[HQ]LSG, Motif 5 - N[QH]LYHWHPLMPDSF, Motif 1 - FGESM[IV]E[IM]GAPFSLKGL in COX-1, and Motif4 - YVLTSRSHLL, Motif5 - FAFFAQHFTHQFFKT, Motif 1 - GETIKIVIEDY, Motif 2 - EFNTLYHWHPLLPDTPFQI, Motif 3 - GAPFSLKGLMGNPICPEYWKPSTFGGEGVGFKI in COX-2 were found to be totally conserved within species and also containing the active binding residues. As per earlier evidences PMID 10811226 and PMID 7552725 it has been found that Leu119, Phe207, Ile347, Try350, Val351, Ser354, Try356, Phe382, Try386, Trp388, Phe520, Met524, Gly528, Ala 529, Ser532, Ile533, Leu536 for COX-1 and Leu103, Phe191, Ile331, Try334, Val335, Ser339, Try341, Try371, Trp373, Phe504, Met508, Gly512, Ala513, Ser516, Leu517, Leu520 for COX-2 represented as substrate binding site. Metal binding site was reported in COX proteins as Try150, Ala201, Gln205, Gln210, Phe212, Lys213, Thr214, Leu297, Asn384, Try387, His388, Trp389, His390, Met393, Leu410, His448, Val449, Asp552 for COX-1 and In case of COX-2 Try134, Ala185, Gln189, Phe191, Gln194, Phe196, Lys197, Thr198, Asn386, Try389, His390, Trp391, His292, Leu393.

Based on protein-drug interaction it has been confirmed that salicin docked and interacted with polar residues- Glu205, Thr208, His 209, 390, hydrophobic residues - Ala204, His209, Tyr387, His390, Leu392

and Met393, pi-pi level interactions with TRP389 residue and cation-pi interaction containing residues His209 and His390 for COX-1. In the case of COX-2 polar residues-Thr192, His193, Asn368, His372, His374, hydrophobic residues His193, His372, Leu377, pi-pi level interactions with His374 and cation-pi interaction containing residues His193, Phe196, Tyr371 showed better inhibitory activity with salicin. Loll et al. [67] reported that COX-1 (1CQE) receptor are showing interaction complex with HEME (protoporphyrin is containing Fe) ligand, in which Ala167, Gln171, His175, Try353, His354, Trp355 and His356 residues are involved. Kiefer et al. [81] observed that in the case of COX-2 (1CVU) interaction complex with BOG (b-octylglucoside) ligand Ala168, Gln172, Phe174, Try354, His355, Trp356, Leu359 and Leu360 residues act as a catalytic active binding sites. In case of salicin docking interaction with COX-1 and COX-2 it has been found that Ala201, Gln205, Try387, His388, Trp389, His390, Met393 residues of COX-1, and Ala185, Gln189, Try389, His390, Trp391, His292, Leu393 residues of COX-2 involved in interaction. These interacting residues are present in Motif 2 and 5 for both COX proteins and also found conserved in alignment pattern.

Hillarp et al. [82] reported that in case of mutations within the COX-1 gene in aspirin non-responders with recurrence of stroke and carriers and non-carriers of one of the mutations behaved similarly when aggregation and granule content release function were studied using collagen, ADP and arachidonic acid as agonists. Thus their hypothesis do not support that common variants of the COX-1 gene results in unblocked COX-1 molecules in aspirin non-responders.

The present study illustrated the effect of isolated compound salicin from *D. gangeticum* leaves on EAC bearing mice, which significantly increased the life span of treated animal as compared to the EAC control. The reliable conditions for evaluating the value of any anticancer drug are prolongation of life span and decrease in the WBC count [83]. The ascitic fluid is the direct nutritional source to tumor cells and the rapid increase in ascitic fluid with tumor growth could possibly be a means to meet more nutritional requirements of tumor cells [84]. Furthermore the reduced volume of EAC and increased survival time of mice suggest the delaying impact of extracts on cell division [85]. The treatment with salicin inhibited the tumor volume, viable cell count and enhanced survival time of EAC bearing mice. These finding suggest the anti-tumor effects of salicin compound against EAC cell line.

Conclusion

The protein-ligand interaction plays a significant role in structural based drug designing. It has been clearly demonstrated that the approach utilized in this study is successful in finding novel anticancer inhibitor from medicinal plant *D. gangeticum*. The ligand salicin, in particular, from *D. gangeticum* showed high binding affinity against COX-2 protein (PDB ID: PM0077493) (-5 Kcal/mol) and lesser interaction with COX-1 (PDB ID: PM0077492) (-3.79 Kcal/mol) based on docking score. Therefore, this study states the importance of natural plant compound protein-ligand interaction studies, *in silico*. From the docking results, we conclude that salicin could be a potential COX inhibitor. Arachidonic acid (mmu00590) and VEGF signaling (mmu04370) pathway key enzymes play an important role during tumor angiogenesis and metastasis in context of COX proteins so it is possible that proteins related to these metabolisms are actively involved in interaction with salicin. However, additional biological and mutational studies would help in prediction of anti-cancerous compounds. The obtained results are useful to understand the structural features inhibitory activities to COX proteins. The extraction, isolation

and characterization of bioactive compound salicin from leaves of this plant and its *in vivo* anticancer activity confirm salicin as potent anticancer drug.

Acknowledgement

The author P.S. wish to thank ICMR, New Delhi for providing financial assistance as SRF. Department of Chemistry, Banaras Hindu University, Varanasi, India, are acknowledged for recording NMR spectra. P.S. is also thankful to Dr. Vinod Tiwari for providing lab facility and guidance for extraction of plant and Dr. Santosh Kumar Singh for providing animal house facility. P.S. is also thankful to Centre of Experimental Medicine & Surgery, BHU, Varanasi for providing animal house facility to perform all experimentation.

References

1. Samuelsson G (2004) Drugs of Natural Origin: a Textbook of Pharmacognosy, 5th Swedish Pharma Press, Stockholm, Sweden.
2. Balick MJ, Cox PA (1997) Plants, People, and Culture: the Science of Ethnobotany. Scientific American Library, New York, NY, USA.
3. (2001) Pharmacognosy in the 21st century. J Pharm Pharmacol 53: 135-148.
4. Newman DJ, Cragg GM, Snader KM (2000) The influence of natural products upon drug discovery. Nat Prod Rep 17: 215-234.
5. Butler MS (2004) The role of natural product chemistry in drug discovery. J Nat Prod 67: 2141-2153.
6. Ley SV, Baxendale IR (2002) New tools and concepts for modern organic synthesis. Nat Rev Drug Discov 1: 573-586.
7. Geysen HM, Schoenen F, Wagner D, Wagner R (2003) Combinatorial compound libraries for drug discovery: an ongoing challenge. Nat Rev Drug Discov 2: 222-230.
8. Lombardino JG, Lowe JA 3rd (2004) The role of the medicinal chemist in drug discovery--then and now. Nat Rev Drug Discov 3: 853-862.
9. Newman DJ, Cragg GM, Snader KM (2000) The influence of natural products upon drug discovery. Nat Prod Rep 17: 215-234.
10. Bray F, Møller B (2006) Predicting the future burden of cancer. Nat Rev Cancer 6: 63-74.
11. Anand P, Kunnumakkara AB, Sundaram C, Harikumar KB, Tharakan ST, et al. (2008) Cancer is a preventable disease that requires major lifestyle changes. Pharm Res 25: 2097-2116.
12. Federsel HJ (2003) Logistics of process R&D: transforming laboratory methods to manufacturing scale. Nat Rev Drug Discov 2: 654-664.
13. Piggott AM, Karuso P (2004) Quality, not quantity: the role of natural products and chemical proteomics in modern drug discovery. Comb Chem High Throughput Screen 7: 607-630.
14. Tan DS (2004) Current progress in natural product-like libraries for discovery screening. Comb Chem High Throughput Screen 7: 631-643.
15. Koehn FE, Carter GT (2005) The evolving role of natural products in drug discovery. Nat Rev Drug Discov 4: 206-220.
16. FitzGerald GA, Patrono C (2001) The coxibs, selective inhibitors of cyclooxygenase-2. N Engl J Med 345: 433-442.
17. Méric JB, Rottey S, Olaussen K, Soria JC, Khayat D, et al. (2006) Cyclooxygenase-2 as a target for anticancer drug development. Crit Rev Oncol Hematol 59: 51-64.
18. Liu CH, Chang SH, Narko K, Trifan OC, Wu MT, et al. (2001) Overexpression of cyclooxygenase-2 is sufficient to induce tumorigenesis in transgenic mice. J Biol Chem 276: 18563-18569.
19. Subbaramaiah K, Dannenberg AJ (2003) Cyclooxygenase 2: a molecular target for cancer prevention and treatment. Trends Pharmacol Sci 24: 96-102.
20. Brown JR, DuBois RN (2005) COX-2: a molecular target for colorectal cancer prevention. J Clin Oncol 23: 2840-2855.
21. Dempke W, Rie C, Grothey A, Schmoll HJ (2001) Cyclooxygenase-2: a novel target for cancer chemotherapy? J Cancer Res Clin Oncol 127: 411-417.
22. Sorokin A (2004) Cyclooxygenase-2: potential role in regulation of drug efflux and multidrug resistance phenotype. Curr Pharm Des 10: 647-657.

23. Fantappiè O, Masini E, Sardi I, Raimondi L, Bani D, et al. (2002) The MDR phenotype is associated with the expression of COX-2 and iNOS in a human hepatocellular carcinoma cell line. *Hepatology* 35: 843-852.
24. DuBois RN, Radhika A, Reddy BS, Entingh AJ (1996) Increased cyclooxygenase-2 levels in carcinogen-induced rat colonic tumors. *Gastroenterology* 110: 1259-1262.
25. Shiff SJ, Rigas B (1999) The role of cyclooxygenase inhibition in the antineoplastic effects of nonsteroidal antiinflammatory drugs (NSAIDs). *J Exp Med* 190: 445-450.
26. Hao X, Bishop AE, Wallace M, Wang H, Willcocks TC, et al. (1999) Early expression of cyclo-oxygenase-2 during sporadic colorectal carcinogenesis. *J Pathol* 187: 295-301.
27. Thun MJ, Henley SJ, Patrono C (2002) Nonsteroidal anti-inflammatory drugs as anticancer agents: mechanistic, pharmacologic, and clinical issues. *J Natl Cancer Inst* 94: 252-266.
28. Pommery N, Taverne T, Telliez A, Goossens L, Charlier C, et al. (2004) New COX-2/5-LOX inhibitors: apoptosis-inducing agents potentially useful in prostate cancer chemotherapy. *J Med Chem* 47: 6195-6206.
29. Peek RM Jr (2004) Prevention of colorectal cancer through the use of COX-2 selective inhibitors. *Cancer Chemother Pharmacol* 54: S50-S56.
30. Lu X, Xie W, Reed D, Bradshaw WS, Simmons DL (1995) Nonsteroidal antiinflammatory drugs cause apoptosis and induce cyclooxygenases in chicken embryo fibroblasts. *Proc Natl Acad Sci U S A* 92: 7961-7965.
31. Higuchi T, Iwama T, Yoshinaga K, Toyooka M, Taketo MM, et al. (2003) A randomized, double-blind, placebo-controlled trial of the effects of rofecoxib, a selective cyclooxygenase-2 inhibitor, on rectal polyps in familial adenomatous polyposis patients. *Clin Cancer Res* 9: 4756-4760.
32. Chopra RN, Nayar SL, Chopra IC (1956) *Glossary of Indian Medicinal Plants*, CSIR, New Delhi, India.
33. Bakshi DNG, Sensarma P, Pal DC (2001) *A lexicon of medicinal plants in India*. Naya Prakash, Calcutta. 2: 52-53.
34. Trout K (2004) Trout's notes on the Genus *Desmodium*: Trout note #2. Myriatre Production.
35. Jabbar S, Khan MT, Choudhuri MS (2001) The effects of aqueous extracts of *Desmodium gangeticum* DC. (Leguminosae) on the central nervous system. *Pharmazie* 56: 506-508.
36. Rathi A, Rao ChV, Ravishankar B, De S, Mehrotra S (2004) Anti-inflammatory and anti-nociceptive activity of the water decoction *Desmodium gangeticum*. *J Ethnopharmacol* 95: 259-263.
37. Mishra PK, Singh N, Ahmad G, Dube A, Maurya R (2005) Glycolipids and other constituents from *Desmodium gangeticum* with antileishmanial and immunomodulatory activities. *Bioorg Med Chem Lett* 15: 4543-4546.
38. Iwu MM, Jackson JE, Tally JD, Klayman DL (1992) Evaluation of plant extracts for antileishmanial activity using a mechanism-based radiorespirometric microtechnique (RAM). *Planta Med* 58: 436-441.
39. Dharmani P, Mishra PK, Maurya R, Chauhan VS, Palit G (2005) *Desmodium gangeticum*: a potent anti-ulcer agent. *Indian J Exp Biol* 43: 517-521.
40. Govindarajan R, Vijayakumar M, Rao ChV, Shirwaikar A, Kumar S, et al. (2007) Antiinflammatory and antioxidant activities of *Desmodium gangeticum* fractions in carrageenan-induced inflamed rats. *Phytother Res* 21: 975-979.
41. Jain V, Prasad V, Pandey RS (2006) Wound healing activity of *Desmodium gangeticum* in different wound models. *J Plant Sci* 1: 247-53.
42. Purushotaman KK, Kishore VM, Narayanaswamy V, Conolly JD (1971) The Structure and stereochemistry of gangetin, a new pterocarpan from *Desmodium gangeticum* (Leguminosae). *J Chem Soc* 13: 2420-2422.
43. Govindarajan R, Rastogi S, Vijayakumar M, Shirwaikar A, Rawat AK, et al. (2003) Studies on the antioxidant activities of *Desmodium gangeticum*. *Biol Pharm Bull* 26: 1424-1427.
44. Behari M, Varshney A (1986) Sterols from *Desmodium* species. *Indian Drugs* 23: 434-435.
45. Ghosal S, Bhattacharya SK (1972) *Desmodium* alkaloids. II. Chemical and pharmacological evaluation of *D. gangeticum*. *Planta Med* 22: 434-440.
46. Pilotto A, Franceschi M, Longoa MG, Scarcelli C, Orsitto G, et al. (2004) *Helicobacter pylori* infection and the prevention of peptic ulcer with proton pump inhibitors in elderly subjects taking low-dose aspirin. *Dig Liver Dis* 36: 666-670.
47. Hawkey CJ (2004) Non-steroidal anti-inflammatory drugs: who should receive prophylaxis? *Aliment Pharmacol Ther* 20 Suppl 2: 59-64.
48. Bigler J, Whitton J, Lampe JW, Fosdick L, Bostick RM, et al. (2001) CYP2C9 and UGT1A6 genotypes modulate the protective effect of aspirin on colon adenoma risk. *Cancer Res* 61: 3566-3569.
49. Macarthur M, Sharp L, Hold GL, Little J, El-Omar EM (2005) The role of cytokine gene polymorphisms in colorectal cancer and their interaction with aspirin use in the northeast of Scotland. *Cancer Epidemiol Biomarkers Prev* 14: 1613-1618.
50. (2009) WHO monographs on selected medicinal plants.
51. Nayeem A, Sitkoff D, Krystek S Jr (2006) A comparative study of available software for high-accuracy homology modeling: from sequence alignments to structural models. *Protein Sci* 15: 808-824.
52. Köckenberger W, De Panfilis C, Santoro D, Dahiya P, Rawsthorne S (2004) High resolution NMR microscopy of plants and fungi. *J Microsc* 214: 182-189.
53. Guignard L, Ozawa K, Pursglove SE, Otting G, Dixon NE (2002) NMR analysis of in vitro-synthesized proteins without purification: a high-throughput approach. *FEBS Lett* 524: 159-162.
54. Du Q, Jerz G, Ha Y, Li L, Xu Y, et al. (2005) Semi-industrial isolation of salicin and amygdalin from plant extracts using slow rotary counter-current chromatography. *J Chromatogr A* 1074: 43-46.
55. Wishart DS, Knox C, Guo AC, Eisner R, Young N, et al. (2009) HMDB: a knowledgebase for the human metabolome. *Nucleic Acids Res* 37: D603-D610.
56. Felsenstein J (1985) Confidence limits on phylogenies: An approach using the bootstrap. *Evolution* 39: 783-791.
57. Efron B (1982) The jackknife, the bootstrap, and other resampling plans. Society of Industrial and Applied Mathematics CBMS-NSF Monographs 38.
58. Arber N (2008) Cyclooxygenase-2 inhibitors in colorectal cancer prevention: point. *Cancer Epidemiol Biomarkers Prev* 17: 1852-1857.
59. Marnett LJ, Rowlinson SW, Goodwin DC, Kalgutkar AS, Lanzo CA (1999) Arachidonic acid oxygenation by COX-1 and COX-2. Mechanisms of catalysis and inhibition. *J Biol Chem* 274: 22903-22906.
60. Smith WL, Garavito RM, DeWitt DL (1996) Prostaglandin endoperoxide H synthases (cyclooxygenases)-1 and -2. *J Biol Chem* 271: 33157-33160.
61. Kulmacz RJ (1998) Cellular regulation of prostaglandin H synthase catalysis. *FEBS Lett* 430: 154-157.
62. Herschman HR (1996) Prostaglandin synthase 2. *Biochim Biophys Acta* 1299: 125-140.
63. Picot D, Loll PJ, Garavito RM (1994) The X-ray crystal structure of the membrane protein prostaglandin H2 synthase-1. *Nature* 367: 243-249.
64. Luong C, Miller A, Barnett J, Chow J, Ramesha C, et al. (1996) Flexibility of the NSAID binding site in the structure of human cyclooxygenase-2. *Nat Struct Biol* 3: 927-933.
65. Bakhle YS (2001) COX-2 and cancer: a new approach to an old problem. *Br J Pharmacol* 134: 1137-1150.
66. Dannhardt G, Kiefer W (2001) Cyclooxygenase inhibitors--current status and future prospects. *Eur J Med Chem* 36: 109-126.
67. Loll PJ, Garavito RM, Carrell CJ, Carrell HL (1996) 2-bromoacetoxybenzoic acid, a brominated aspirin analog. *Acta Crystallogr C* 52: 375-377.
68. Kurumbail RG, Stevens AM, Gierse JK, McDonald JJ, Stegeman RA, et al. (1996) Structural basis for selective inhibition of cyclooxygenase-2 by anti-inflammatory agents. *Nature* 384: 644-648.
69. Ermondi G, Caron G, Lawrence R, Longo D (2004) Docking studies on NSAID/COX-2 isozyme complexes using contact statistics analysis. *J Comput Aided Mol Des* 18: 683-696.
70. Singh P, Bhardwaj A (2010) Mono-, di-, and triaryl substituted tetrahydropyrans as cyclooxygenase-2 and tumor growth inhibitors. Synthesis and biological evaluation. *J Med Chem* 53: 3707-3717.

71. Taylor RD, Jewsbury PJ, Essex JW (2002) A review of protein-small molecule docking methods. J Comput Aided Mol Des 16: 151-166.
72. Schulz-Gasch T, Stahl M (2003) Binding site characteristics in structure-based virtual screening: evaluation of current docking tools. J Mol Model 9: 47-57.
73. Wang R, Lu Y, Wang S (2003) Comparative evaluation of 11 scoring functions for molecular docking. J Med Chem 46: 2287-2303.
74. Ferrara P, Gohlke H, Price DJ, Klebe G, Brooks CL 3rd (2004) Assessing scoring functions for protein-ligand interactions. J Med Chem 47: 3032-3047.
75. Vane JR, Flower RJ, Botting RM (1990) History of aspirin and its mechanism of action. Stroke 21: IV12-23.
76. Akao T, Yoshino T, Kobashi K, Hattori M (2002) Evaluation of salicin as an antipyretic prodrug that does not cause gastric injury. Planta Med 68: 714-718.
77. Ashwin KA, Bairy KL, Vidyasagar S, Verma M, Prashanth CK, et al. (2007) Aspirin resistance. Indian J Physiol Pharmacol 51: 109-117.
78. Kurogi Y, Güner OF (2001) Pharmacophore modeling and three-dimensional database searching for drug design using catalyst. Curr Med Chem 8: 1035-1055.
79. Oshiro CM, Kuntz ID, Dixon JS (1995) Flexible ligand docking using a genetic algorithm. J Comput Aided Mol Des 9: 113-130.
80. Willard L, Ranjan A, Zhang H, Monzavi H, Boyko RF, et al. (2003) VADAR: a web server for quantitative evaluation of protein structure quality. Nucleic Acids Res 31: 3316-3319.
81. Kiefer JR, Pawlitz JL, Moreland KT, Stegeman RA, Hood WF, et al. (2000) Structural insights into the stereochemistry of the cyclooxygenase reaction. Nature 405: 97-101.
82. Hillarp A, Palmqvist B, Lethagen S, Villoutreix BO, Mattiasson I (2003) Mutations within the cyclooxygenase-1 gene in aspirin non-responders with recurrence of stroke. Thromb Res 112: 275-283.
83. OBERLING C, GUERIN M (1954) The role of viruses in the production of cancer. Adv Cancer Res 2: 353-423.
84. Prasad SB, Giri A (1994) Antitumor effect of cisplatin against murine ascites Dalton's lymphoma. Indian J Exp Biol 32: 155-162.
85. Sur P, Bag SP, Sur B, Khanam JA (1997) Chloroaceto hydroxamic acid as antitumor agent against Ehrlich ascites carcinoma in mice. Neoplasma 44: 197-201.